Studies on silica and metallic nanoparticles and their possible use for bio-medical applications

K. Das and P. K. Gupta
Laser Bio-Medical Applications & Instrumentation Division,
Raja Ramanna Center for Advanced Technology,
Indore, M.P. 452013 India

kaustuv@rrcat.gov.in

BIOMEDICAL ACTIVITIES AT RRCAT

Use of light (lasers) for

- **Biomedical Imaging**
- **Diagnosis**
- **Therapy**
- **Manipulation of single cells/sub-cellular objects**

- **Preparation of nanoparticles and exploration of their use for biomedical imaging, diagnosis and therapy**

(http://www.cat.ernet.in/technology/laser/bmas/research.html)

Imaging by Optical Coherence Tomography

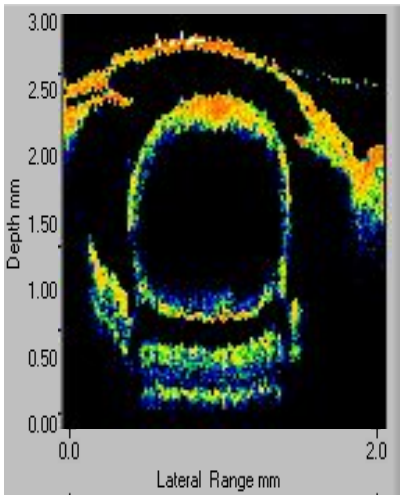

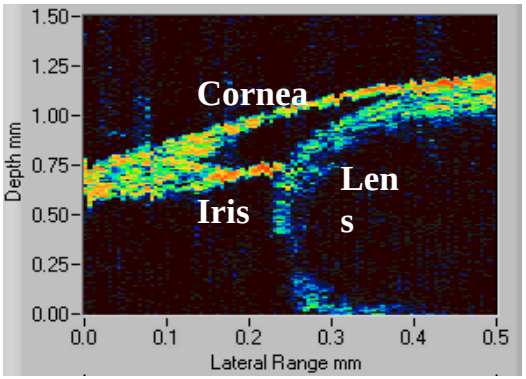

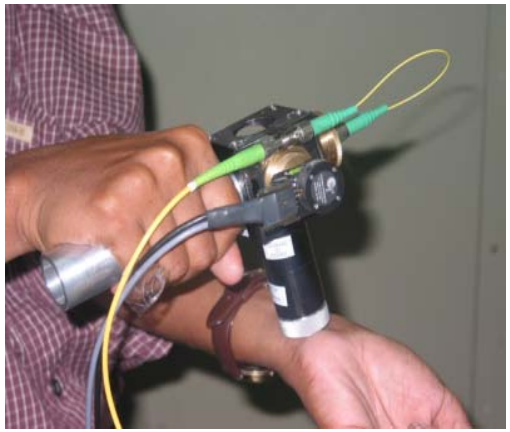

OCT images of Zebra Fish Eye

Current Science, 90, 1506 (2006); Appl. Phys. B 87, 607 (2007)

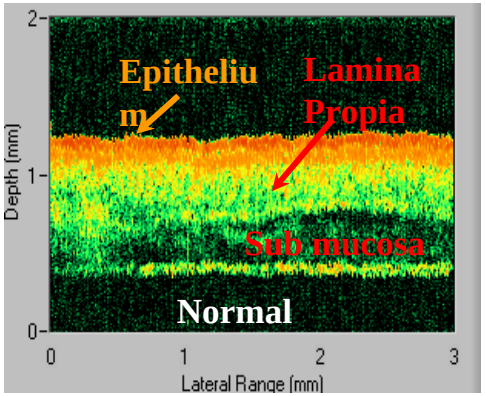

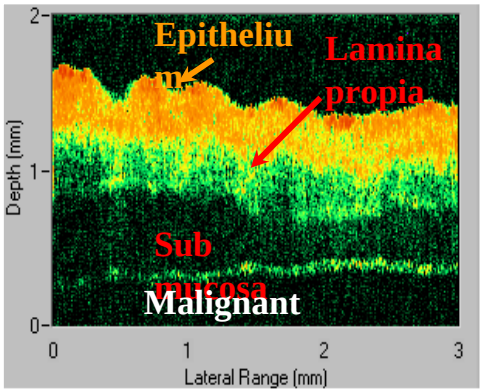

OCT images of (a) normal and (b) malignant Hamster cheek pouch tissue

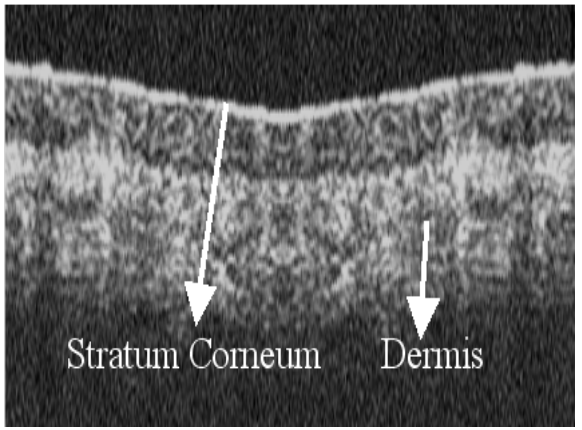

Real time hand held OCT set up for dermatological applications

OPTICAL SPECTROSCOPIC DIAGNOSIS OF CANCER

UNDERSTAND FLUORESCENCE FROM HUMAN TISSUE AND EVALUATE POTENTIAL OF USING IT FOR CANCER DIAGNOSIS

SIGNIFICANT VARIATION IN FLUOROPHORE CONCENTRATION IN N & M

System in use for the diagnosis of cancer of oral cavity

Diagnostic Algorithm	Predictive Accuracy for Validation Data Set	
	Sensitivity (%)	Specificity (%)
PCA	80	58
FLD	73	92
MRDF	95	96
SVM	93	95
RVM	93	95

Lasers Surg. Med., 33, 48 (2003)

J. Biomed. Opt., 10, 024034(2005)

Lasers Surg. Med., 36, 323 (2005)

Multi class Classification:

J Photochem. and Photobiol B, 85, 109 – 117 (2006)

PHOTODYNAMIC THERAPY

Chlorophyl derivatives (CP6, purpurin, …) — *Photochem. Photobiol. 75, 488, (2002),*

Photophysical characterization — *Photochem. Photobiol.Sci., 3, 231(2003)*

Evaluation in cell lines and animal models — *Photochem. Photobiol. Sci. 3,231-235 (2004);…*

Use of CP6 for treatment of tumor in hamster cheek pouch

Oral Oncology , 42, 77-82, (2006)

- Systemic delivery effective in small size tumors
- Topical application more effective for large size tumors (8mm)
- Complete tumor necrosis and regression in small size tumor (<4 mm)
- Superficial necrosis and size reduction in large tumor, complete regression when PDT repeated 3-4 times at 72 hr interval

Photodynamic inactivation of antibiotic resistant bacterial cells

Current Microbiology 50, 277-280 (2005)

Toluidine Blue-Mediated Photodynamic Effects on Staphylococcal Biofilms

Antimicrobial agents and chemotherapy, (2008)

Application of Optical tweezers

BIOPHOTONICS

Rotating Line Optical Tweezers Enables Controlled Intracellular Rotation of Microscopic Objects

Raktim Dasgupta, Samarendra Kumar Mohanty and Pradeep Kumar Gupta

objects. Most of the techniques used for rotation of objects are limited to absorbing, birefringent or specially fabricated structures and hence are not suitable for rotation of biological objects.[1-3] Recently an interferometric approach suitable for rotation of a trapped biological object has been reported.[4] However, this method has two important drawbacks: poor utilization of the trap laser power due to the loss in the generation of the required interference pattern and high susceptibility of the interference pattern to

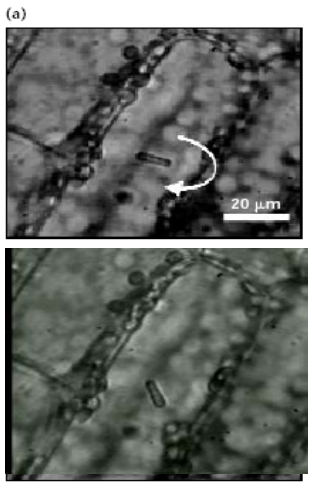

Figure 1. Rotation of an intracellular object insic
line tweezers. The rod shaped structure was trap
speed of 4 Hz. The direction of rotation is shown
45° (b); 145° (c); and 235° (d). All the images w

BIOPHOTONICS

Nanosecond Near-Infrared Laser-Assisted Microinjection Into Targeted Cells

Samarendra Kumar Mohanty, Mrinalini Sharma and Pradeep Kumar Gupta

siderable attention in the context of a variety of applications in genetics, cell biology and biotechnology. Compared with conventional techniques, optoporation is more efficient, less tedious and offers the advantage of being usable on cells in suspension as well as on attached cells. Because the constituents of the cell membrane have strong absorption in the ultraviolet (UV) spectral range, lasers in this spectral range were the first to be investigated for optoporation. But the use of UV light raises concerns about damage to cells or even about exogenous biological material being transferred into the cell. Use of lasers of wavelength in the near-infrared region would be more

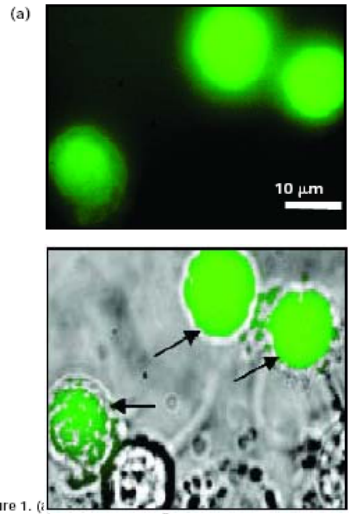

Figure 1. (a
cent protein (GFP) coding plasmid using optoporation with r
laser beam. (b) Bright field and fluorescence images of cells a

Optics & Photonics News, Dec. 2003

Biophotonics

Self-Rotation of Red Blood Cells in Optical Tweezers: Prospects for High Throughput Malaria Diagnosis

Samarendra Kumar Mohanty, Abha Uppal and Pradeep Kumar Gupta

infected red blood cells (RBCs) is more rigid than the membrane of normal RBCs.[2] A measurement of membrane elasticity of a RBC can, therefore, be used for the detection of malaria-infected RBCs.[4] More interestingly, it has been determined[4] that, in a hypertonic buffer medium (> 800-mOsm/kg osmolarity), malaria-infected RBCs either do not rotate at all or rotate at a significantly slower speed because of their rigid membrane. A normal RBC, in contrast, rotates by itself when placed in a laser optical trap at the same trap beam power. This difference in rotational speed has been exploited for the detection of malaria-infected cells.[4]

In a hypertonic buffer, a meniscus-shaped normal RBC rotates when it is optically trapped with trap beam power beyond ~40 mW (Fig. 1) because of the torque that is generated on the cell by the transfer of linear momentum from the

OPTICS IN 2004

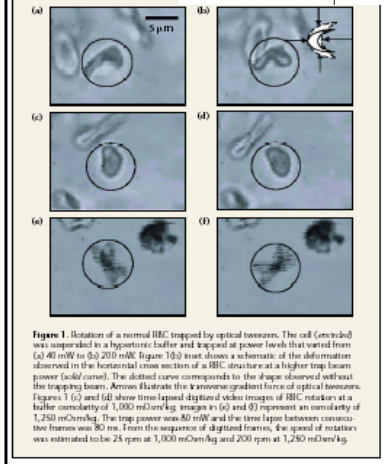

Figure 1. Rotation of a normal RBC trapped by optical tweezers. The cell (encircled) was suspended in a hypertonic buffer and trapped at power levels that varied from (a) 40 mW to (b) 200 mW. Figure 1(b) inset shows a schematic of the deformation observed in the horizontal cross section of a RBC. (c) structure at a higher trap beam power (solid curve). The dotted curve corresponds to the shape observed without the trapping beam. Arrows illustrate the transverse gradient force of optical tweezers. Figures 1 (c) and (d) show time-lapsed digitized video images of RBC rotation at a buffer osmolarity of 1,000 mOsm/kg. Images in (c) and (d) represent an osmolarity of 1,250 mOsm/kg. The trap power was 80 mW and the time lapse between consecutive frames was 80 ms. From the sequence of digitized frames, the speed of rotation was estimated to be 25 rpm at 1,000 mOsm/kg and 200 rpm at 1,280 mOsm/kg.

Optics & Photonics News, Dec. 2004

Transport of Microscopic Objects Using Line Optical Tweezers: Manipulation of Neuronal Growth Cones

BIOPHOTONICS | 2005

Samarendra Kumar Mohanty, Mrinalini Sharma, Mitradas Panicker and Pradeep Kumar Gupta

The transport of microscopic objects plays an important role in several biophysical processes that are crucial for cell functioning. By becoming able to effect controlled transport of intracellular objects, researchers can not only understand these fundamental processes better but also manipulate the functionality of living cells.

We have shown that line optical tweezers, with an asymmetric intensity distribution along the major axis of the elliptical trap beam, can be used for efficient and controlled transport of microscopic objects in a plane transverse to the direction of beam propagation.[1] The asymmetry in the intensity distribution of the trap beam about its center results in a potential well that is asymmetric about the center of the beam.

Thus, particles at the steep end of the potential well are pulled toward the potential minima, accelerate, and are ejected in the direction toward the lower stiffness. Since the gradient force is large and symmetric in the other two orthogonal directions, the particles are constrained to move along the major axis of the line tweezers.

We controlled the depth and the asymmetry of the potential well by a control on trap beam power and by a change in the angle of incidence of the laser beam with respect to the optic axis of the microscope objective. To change the direction of transport, we rotated the cylindrical

gradient end of the elliptical focus such that the tip of the growing edge was closer to the lower gradient force. Since the neuronal growth is believed to involve transport of actins in the direction of the growth cone,[2] the observed enhancement in growth can be attributed to diffusion of actins.

Compared to a growth rate of 1 ± 1 μm/h observed for unexposed neurons, the lamellipodia extension rate in a neuron subjected to line tweezers was estimated to be 32 ± 6 μm/h. The asymmetric transverse gradient force could also be used for induction of new growth cones from the neuronal cell body (see figure). The optically induced growth cones showed branching similar to that observed in the natural process of growth.

However, the growth rate of these induced cones was lower (15 ± 3 μm/h) than that achieved for natural growth cones. This approach could be used to change the orientation of a growth cone to bring it into close proximity with a cone of another neuron. The ability to exert such control on neuronal growth cones may prove useful for establishing a connection between two neurons. ⁂

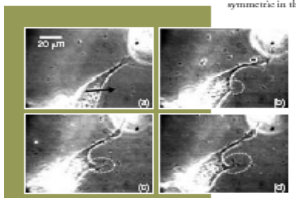

Optics & Photonics News, Dec. 2005

Interaction of organically modified silica nanoparticles with molecules of biomedical relevance

Silica Nanoparticles

Biocompatible & nontoxic

Hydrophilic in nature
(reduces the problems of non-specific binding and clustering)

Chemical inertness & transparency

Less prone to attack from microbes.

Easy to prepare, modify surface and separate via centrifugation

Imaging & Drug delivery

Organically modified SiNPs (~25 nm) were prepared using Vinyl triethoxysilane (VTES) and 3-aminopropyl-triethoxysilane (APTS) using a micellar template

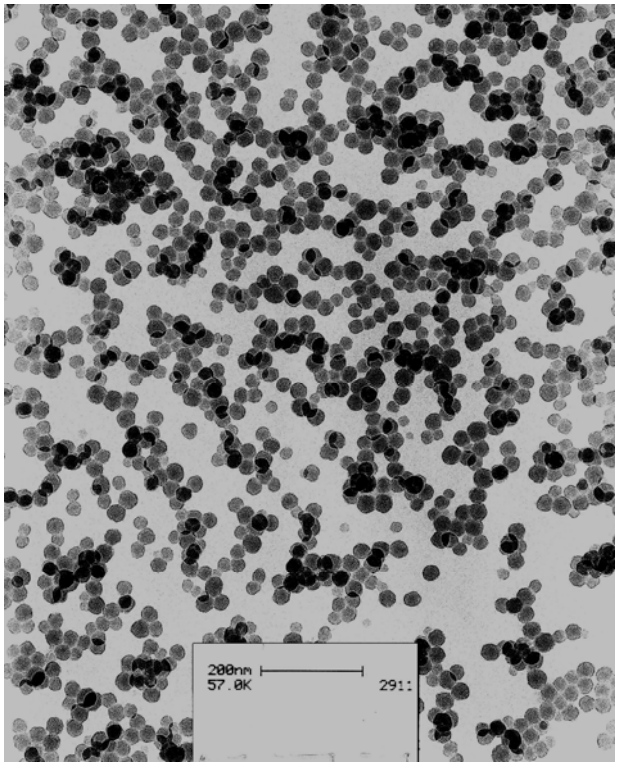

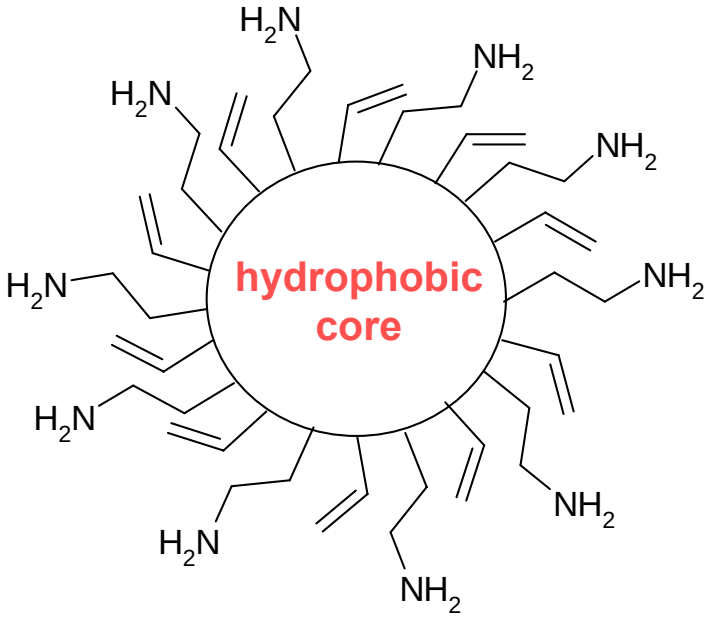

At neutral water the amine groups present at the surface are expected to be positively charged as the pK_a value of the 3-aminopropyl group of APTS is ~ 9

ANS

Polarity sensitive fluorescence probes

TNS

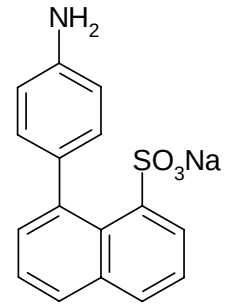

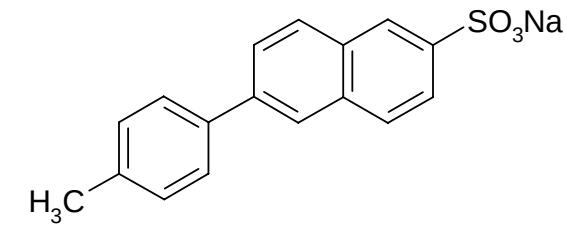

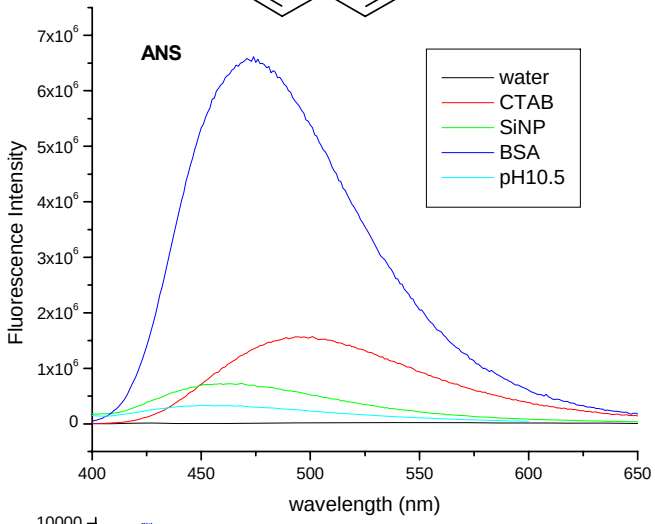

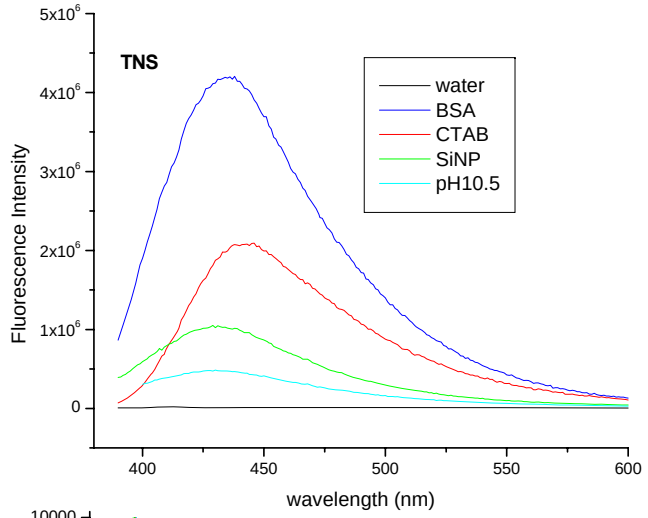

Water

CTAB (micelle)

SiNP (neutral)

SiNP (basic)

BSA (protein)

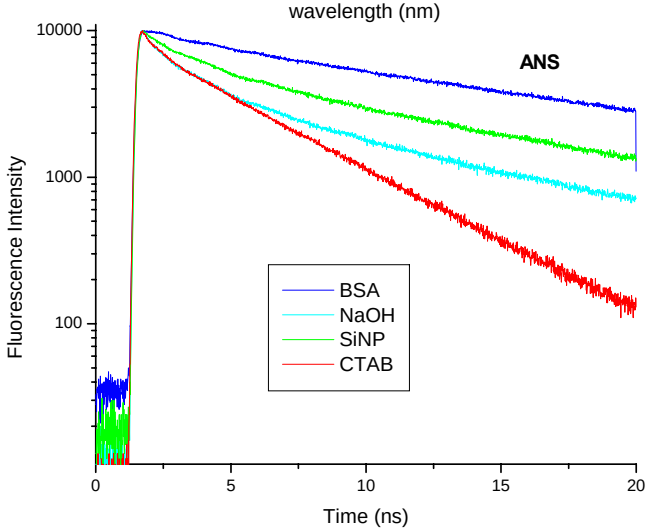

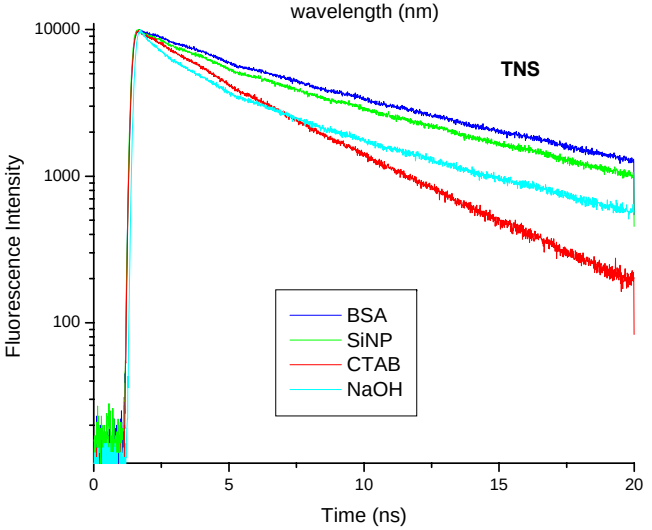

Steady state & time resolved fluorescence

Time resolved polarized fluorescence

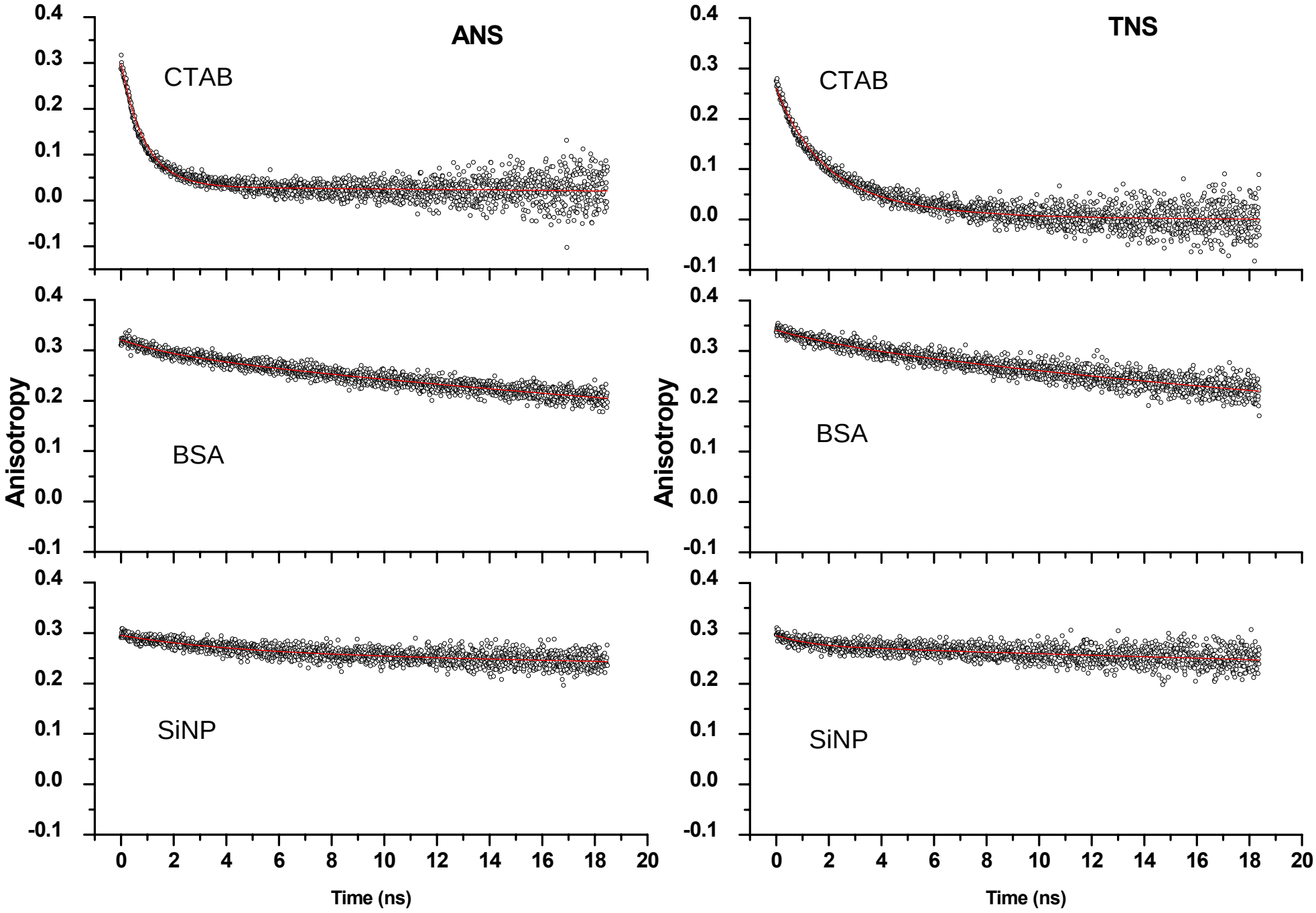

- **A comparison of the photophysical parameters of ANS & TNS in SiNP, protein and micellar environment suggests the presence of fluorescence quenching in SiNP, which might be static in nature.**

- **Both ANS and TNS reside at the interface of CTAB micelles. With SiNP, ANS & TNS resides at interface (electrostatic interaction) and in the core (hydrophobic interaction).**

- **Fluorescence polarization measurements suggests that they are tightly bound to SiNP and protein compared to CTAB micelles.**

polarity

PRODAN

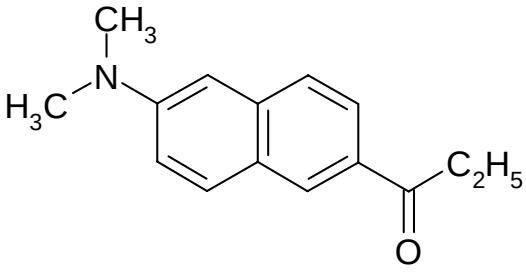

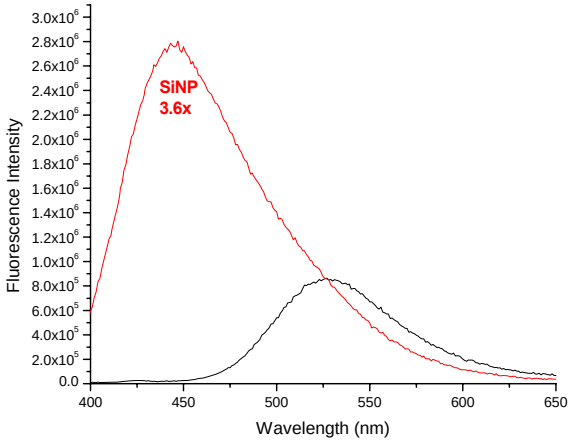

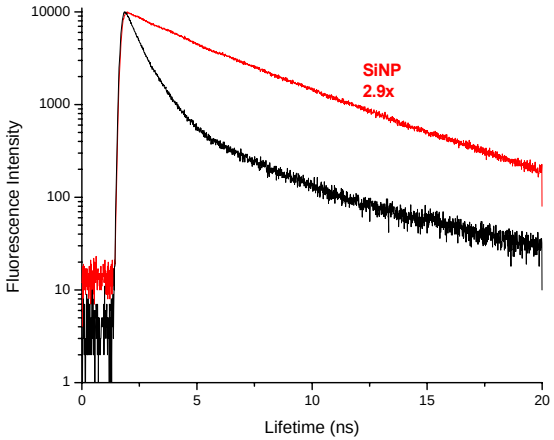

nucleic acid stain

DAPI

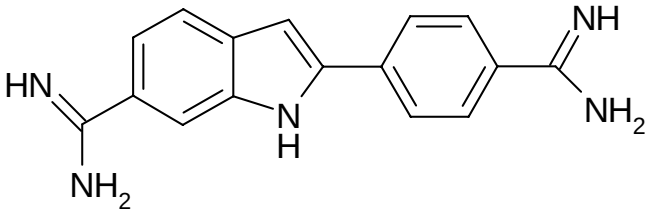

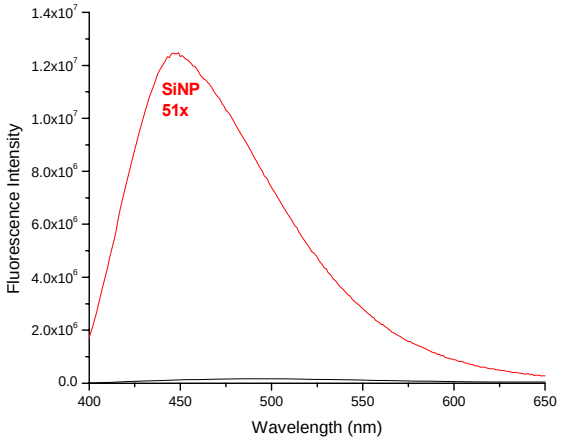

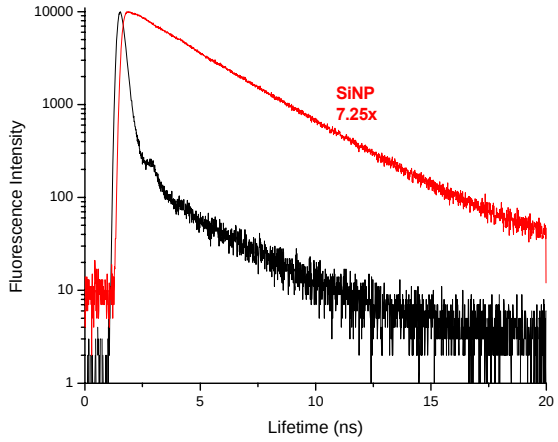

hydrophobic

Nile Red

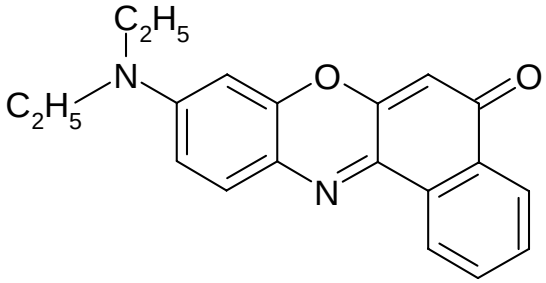

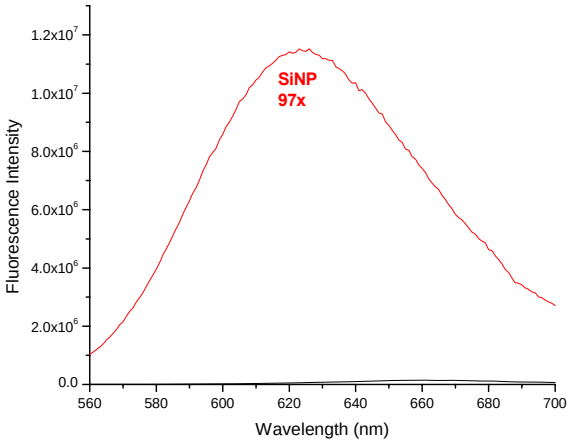

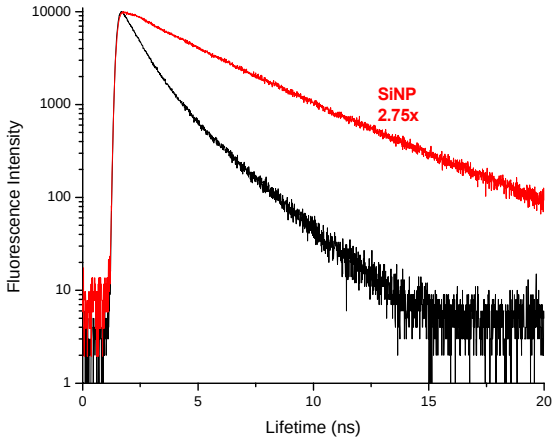

Forster Energy transfer in SiNP

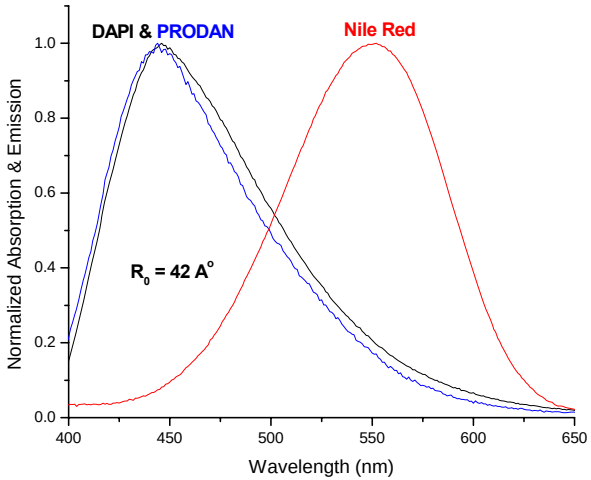

DAPI-Nile Red

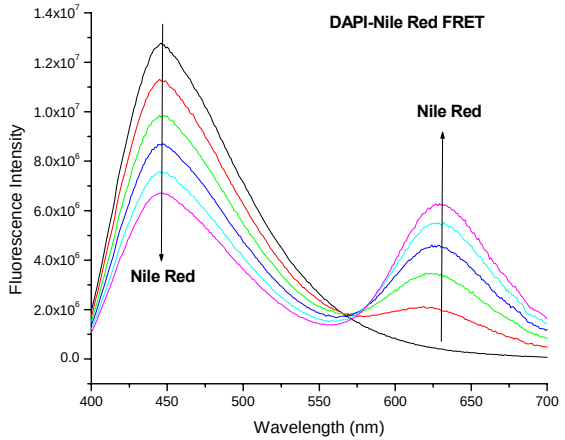

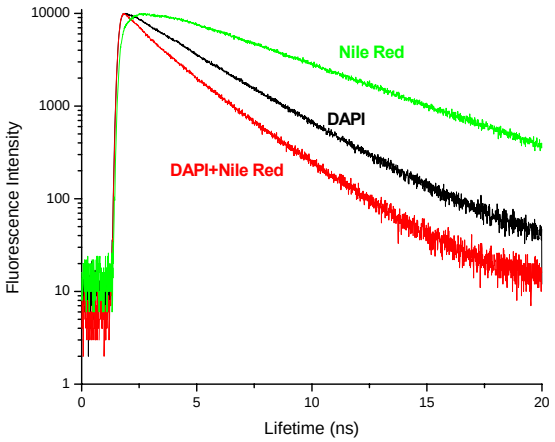

PRODAN-Nile Red

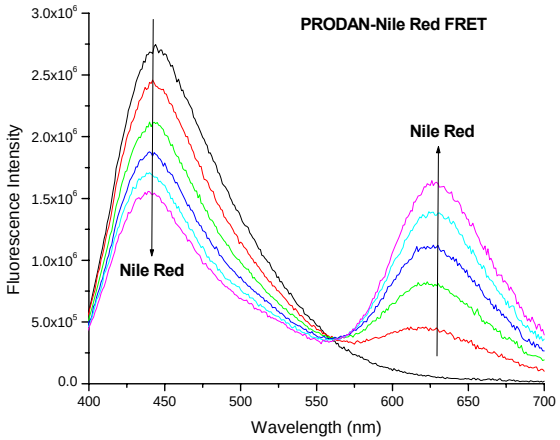

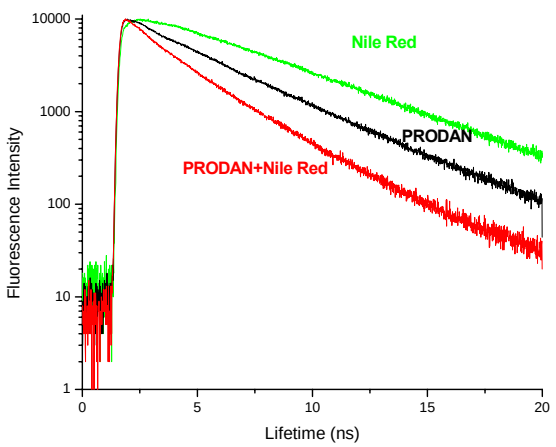

Chlorin-p6

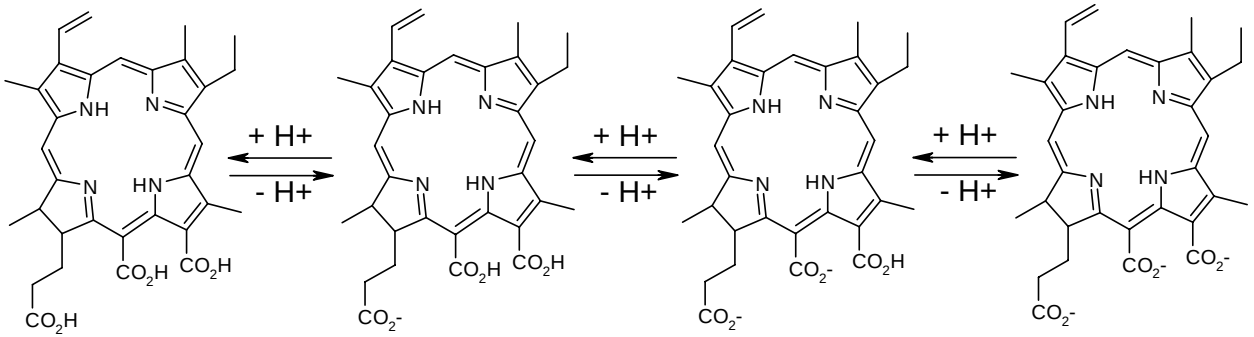

Non-fluorescent aggregates formed at low pH due to successive protonation of the COOH groups

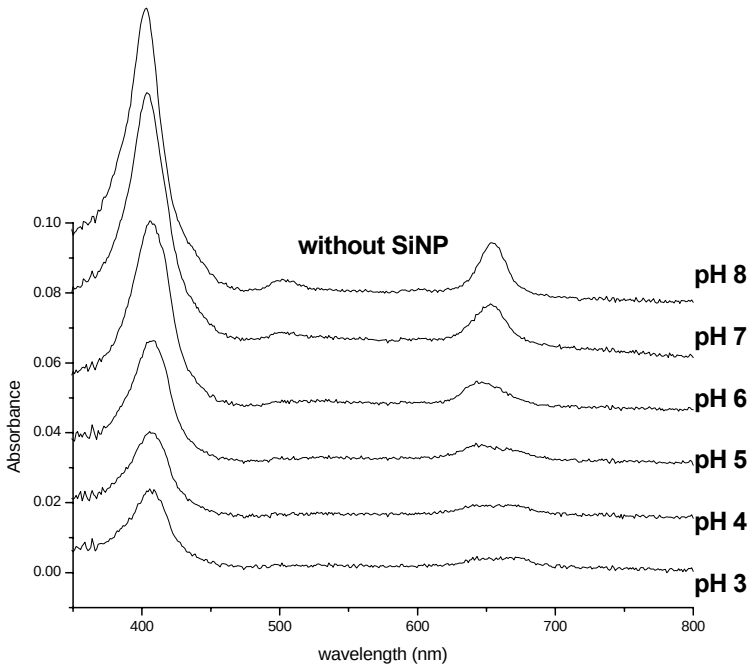

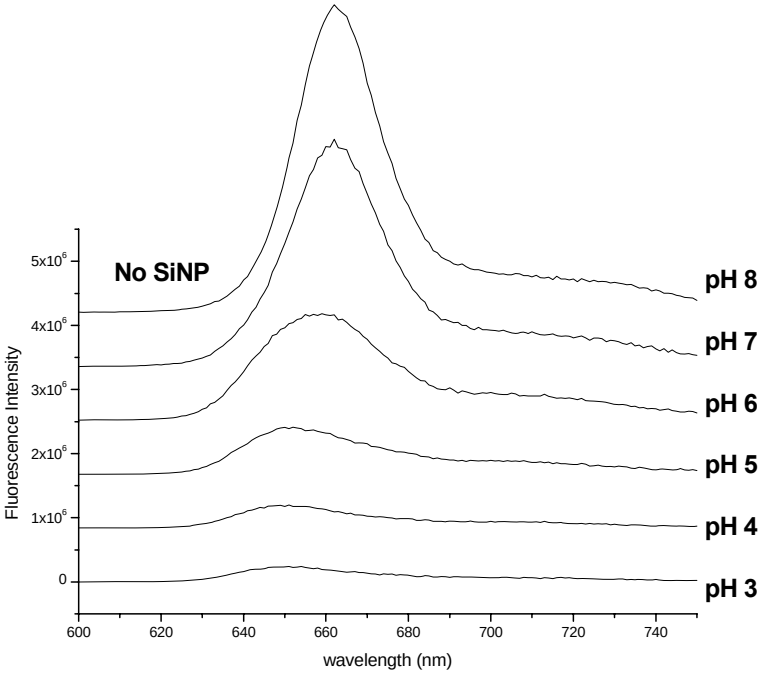

Absorption & emission at different pH

Absorption & emission at different pH with SiNP

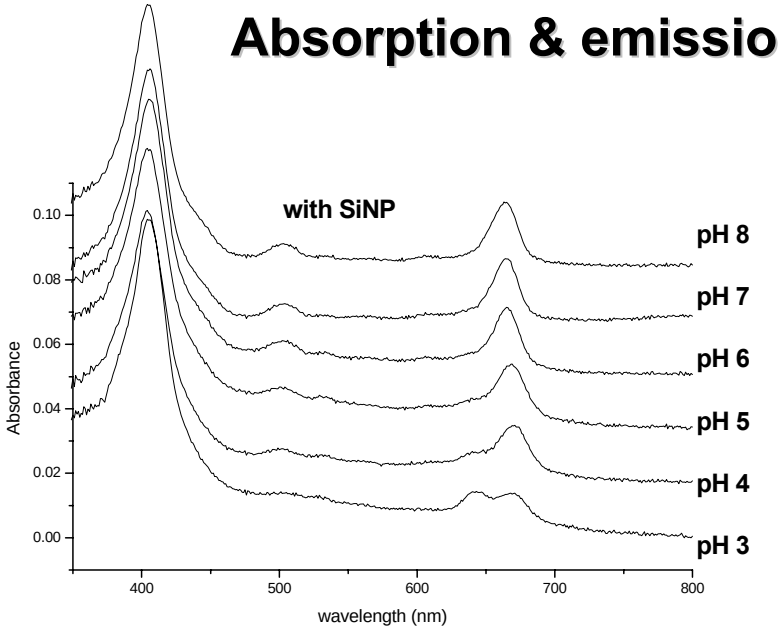

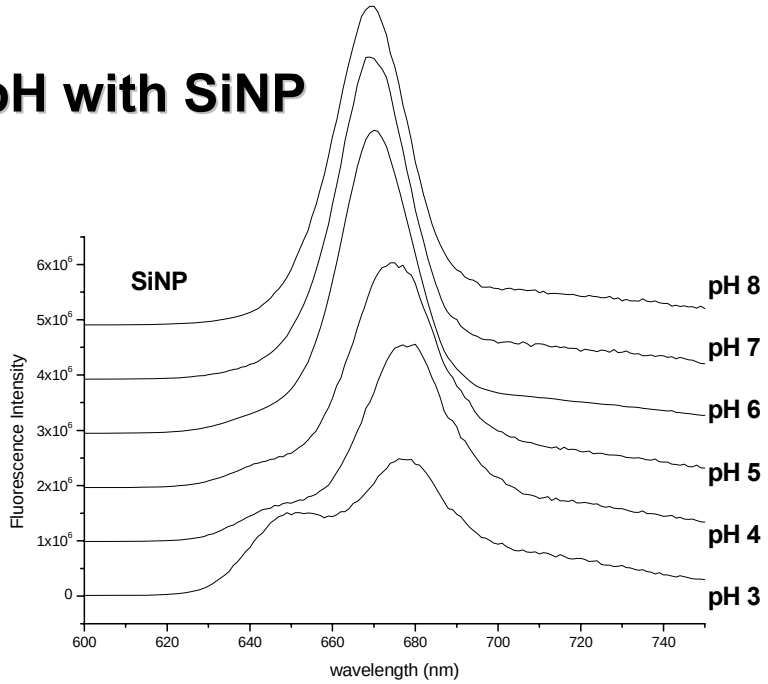

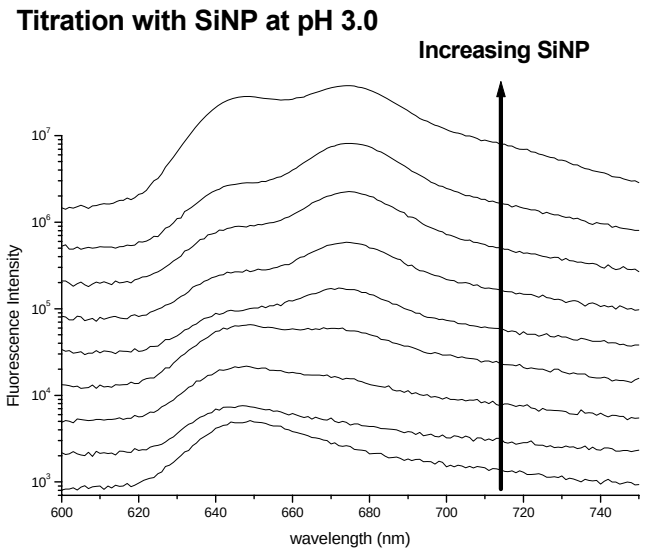

Emission titration with SiNP at pH 3.0

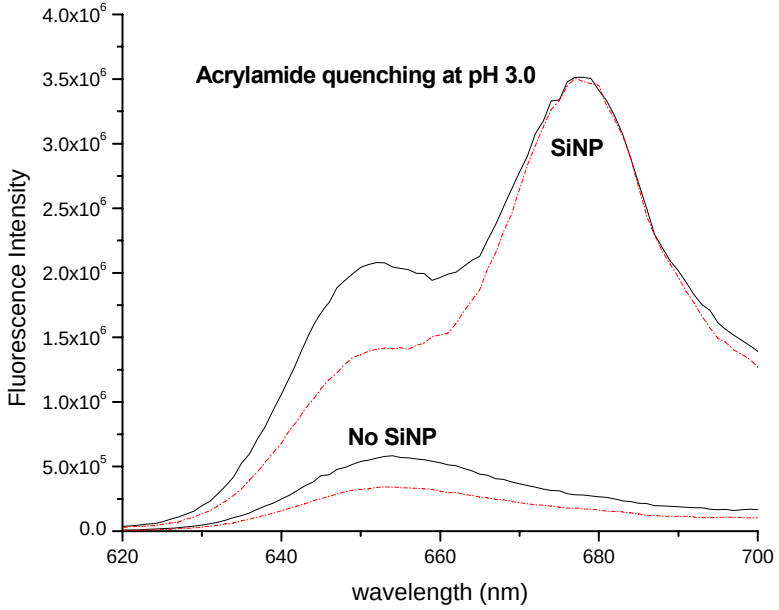

Effect of a quencher

- **Acid-base ionization equilibrium is significantly affected as a result of strong electrostatic binding between the negatively charged drug and SiNP.**

- **The spectroscopic signature of the drug bound to SiNP suggests that the tri-anionic form of the drug remains bound to the positively charged SiNP at pH 8.0.**

- **At pH 5.0 and 3.0 the formation of hydrophobic aggregates is disrupted significantly due to the presence of electrostatic binding force, which competes with intermolecular hydrophobic forces.**

- **The interplay of hydrophobic and electrostatic forces in the drug-nanoparticle binding process might affect the relative uptake and photodynamic efficacy of the free drug and the drug-nanoparticle complex in cancer cells.**

Merocyanine 540

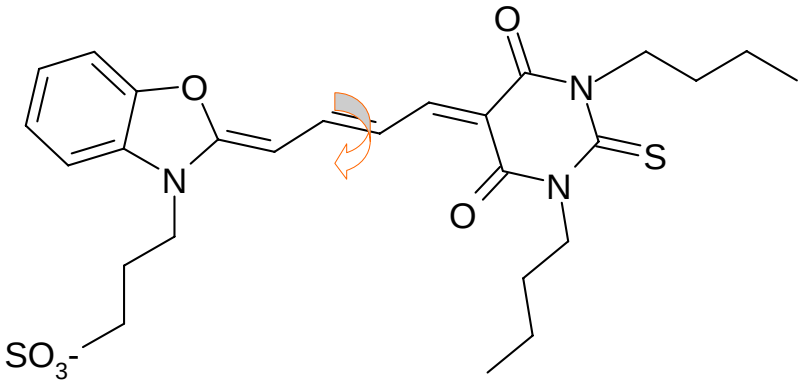

Anionic photosensitizer

Aggregation & photoisomerization
Weakly fluorescent
Photodegradable
Low singlet oxygen quantum yield

} In water

Reduce photoisomerization

Enhance $^1O_2$ yield & photostability?

Binding with liposomes reduces photoisomerization rate and increases $^1O_2$ yield by ~20 times

M. Krieg, *Biochim. Biophys. Acta, 1105, 333 (1992)*

Use positively charged silica nanoparticles (SiNP) to reduce photoisomerization rate??

Interaction between MC540 and SiNPs in aqueous media

Spectroscopic investigation

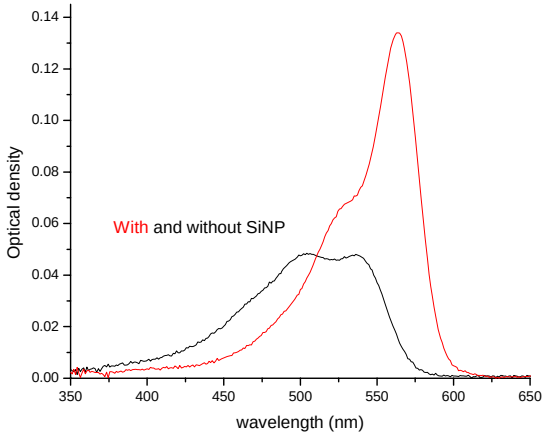

Absorption

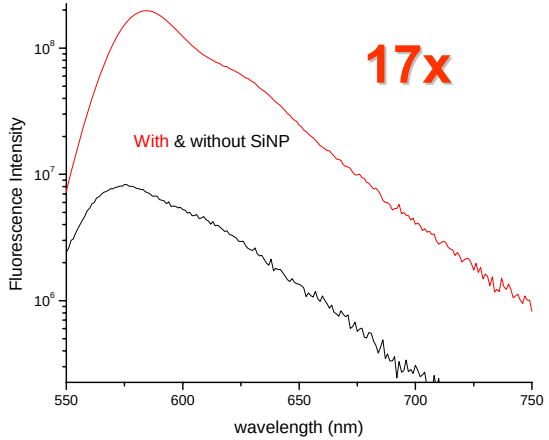

Fluorescence
steady state

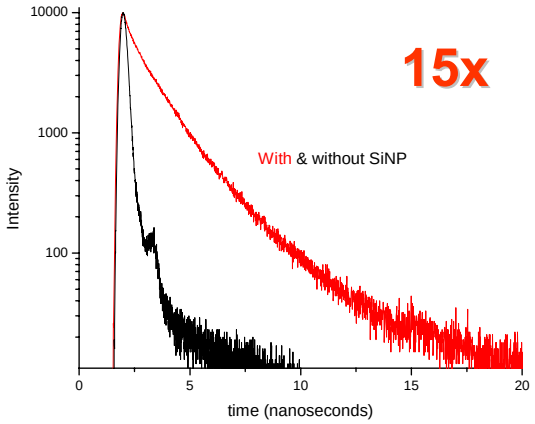

Fluorescence
time resolved

Enhanced absorption and fluorescence in presence of positively charged SiNPs

Fluorescence parameters in different environments

Environment	Absorption	Fluorescence (quantum yield)	Fluorescence lifetime (ns)	Radiative rate ($x10^{-9}$)	Nonradiative rate ($x10^{-9}$)
Water	505/536	570 (0.03)	0.10	0.31	9.70
Liposome	565	583 (0.49)	1.5	0.33	0.34
Water+ SiNP	563	583 (0.53)	1.5	0.36	0.32

Decrease in nonradiative rate ⟹ Increased photostability?

Photobleaching of free dye and dye-SiNP complex

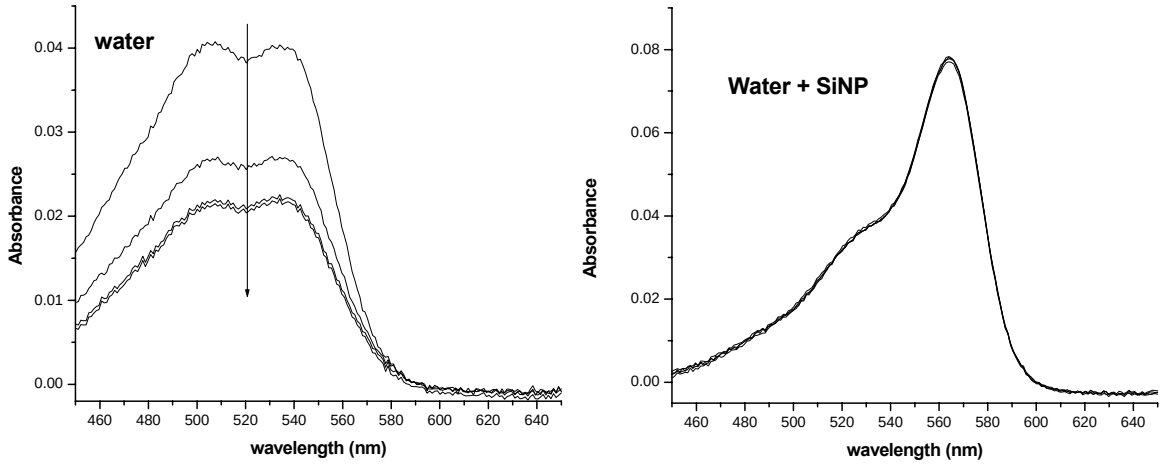

Photostability increases in presence of SiNPs

Cellular uptake & phototoxicity

Target MCF cells

Plated cells in 60 mm petri dish
Incubated in serum free minimum essential media for one hour
(MC540 1µM & SiNP 10-20 µgm/mL)

Cellular uptake

Fluorescence microscopy of free drug & drug-SiNP complex
(Ex = 530 / Em > 590)

Light induced toxicity

Irradiated at 450-650 nm
Light dose: 1.8, 3.6 and 5.4 kJ/m^2)

- **Only MCF cells** **control**
- **MCF cells + drug**
- **MCF cells + SiNP**
- **MCF cells + SiNP-drug complex**

Monitoring cell survival after 24 hours using MTT assay

Cellular uptake : Fluorescence microscopy

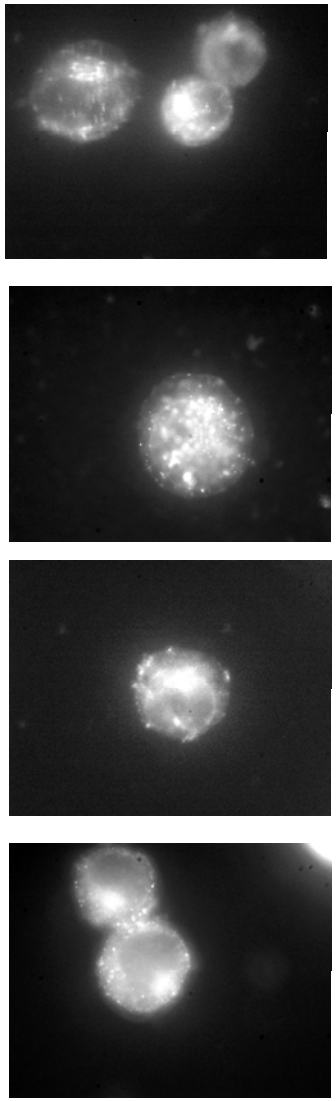

1 µM MC540

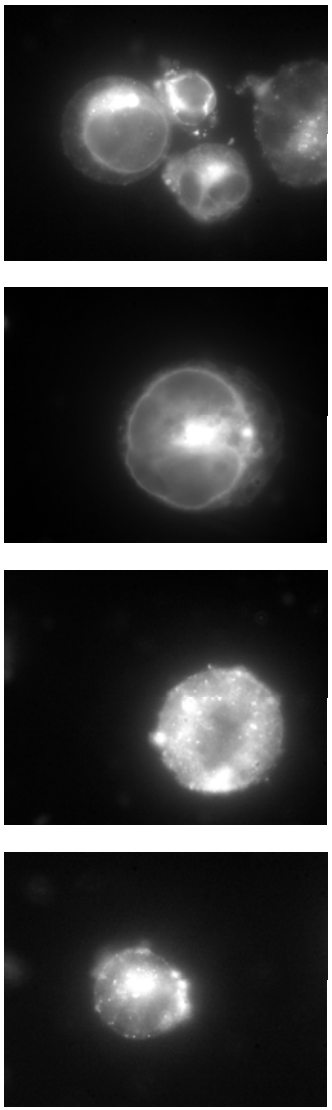

1 µM MC540 + 20 µgm/mL SiNP

Light induced toxicity

(No dark toxicity observed)

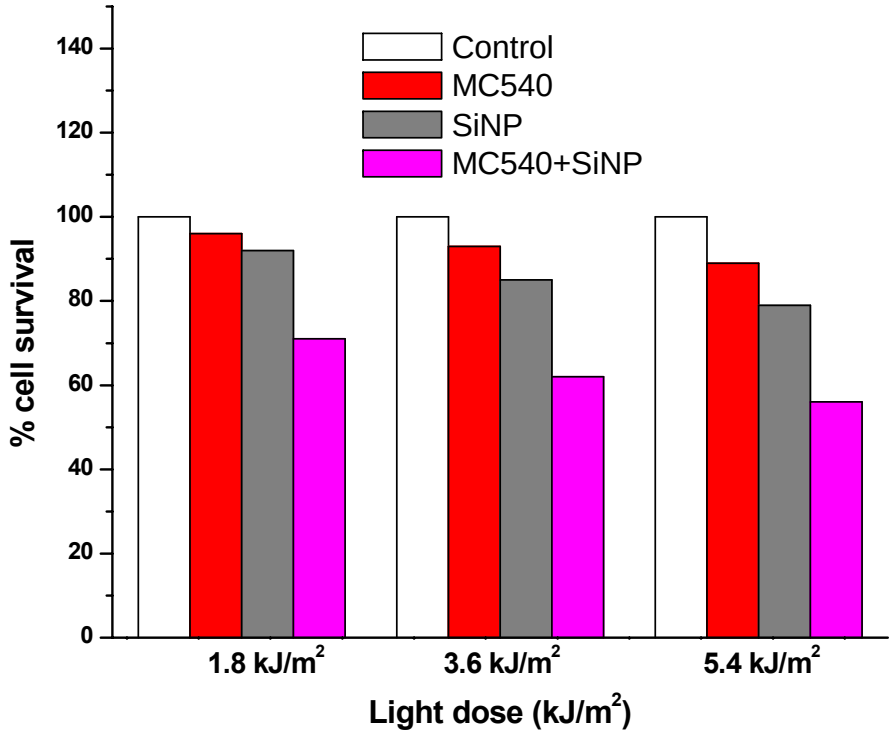

Drug = 1 µM
SiNP = 20 µgm/mL

The light dose dependent cell killing were observed to be the highest for the drug-SiNP complex

Summary

•The electrostatic binding between Merocyanine 540 and SiNPs has been characterized using absorption and fluorescence spectroscopy

•The binding resulted in significant changes in the absorption spectra. The fluorescence intensity and lifetime gets enhanced by more than an order of magnitude

•The results obtained suggest that this is due to the reduced photoisomerization rate of the dye bound to the nanoparticle

•Consistent with the expectation that a reduction in the photoisomerization rate should enhance the singlet oxygen yield of the dye, the light induced toxicity of the dye-nanoparticle complex (tested with MCF cells) was observed to be higher compared to the free dye

Multiphoton-absorption induced processes in silver nanoparticles under femtosecond laser excitation

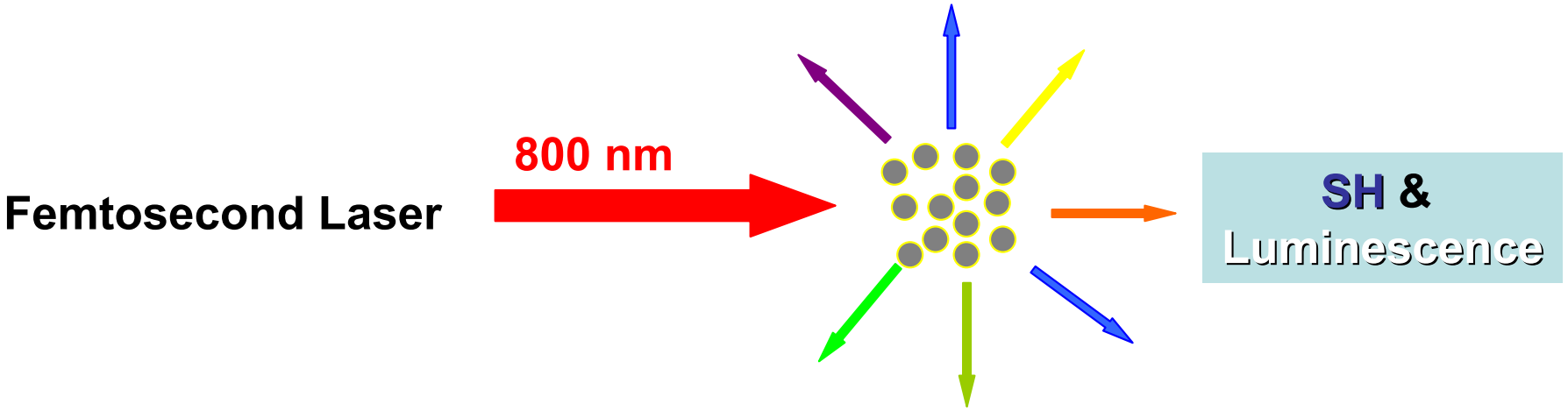

SH generation

$$I_{2\omega} = G < N_s \beta_s^{\ 2} + N_a \beta_a^{\ 2} > I_\omega^2 e^{(-N_a(2\alpha_\omega + \alpha_{2\omega})l)}$$

Luminescence

Radiative electron hole recombination in the interband transitions between the *sp* and *d* bands

Both depends critically on the shape and size of the nanostructures

Experimental Setup

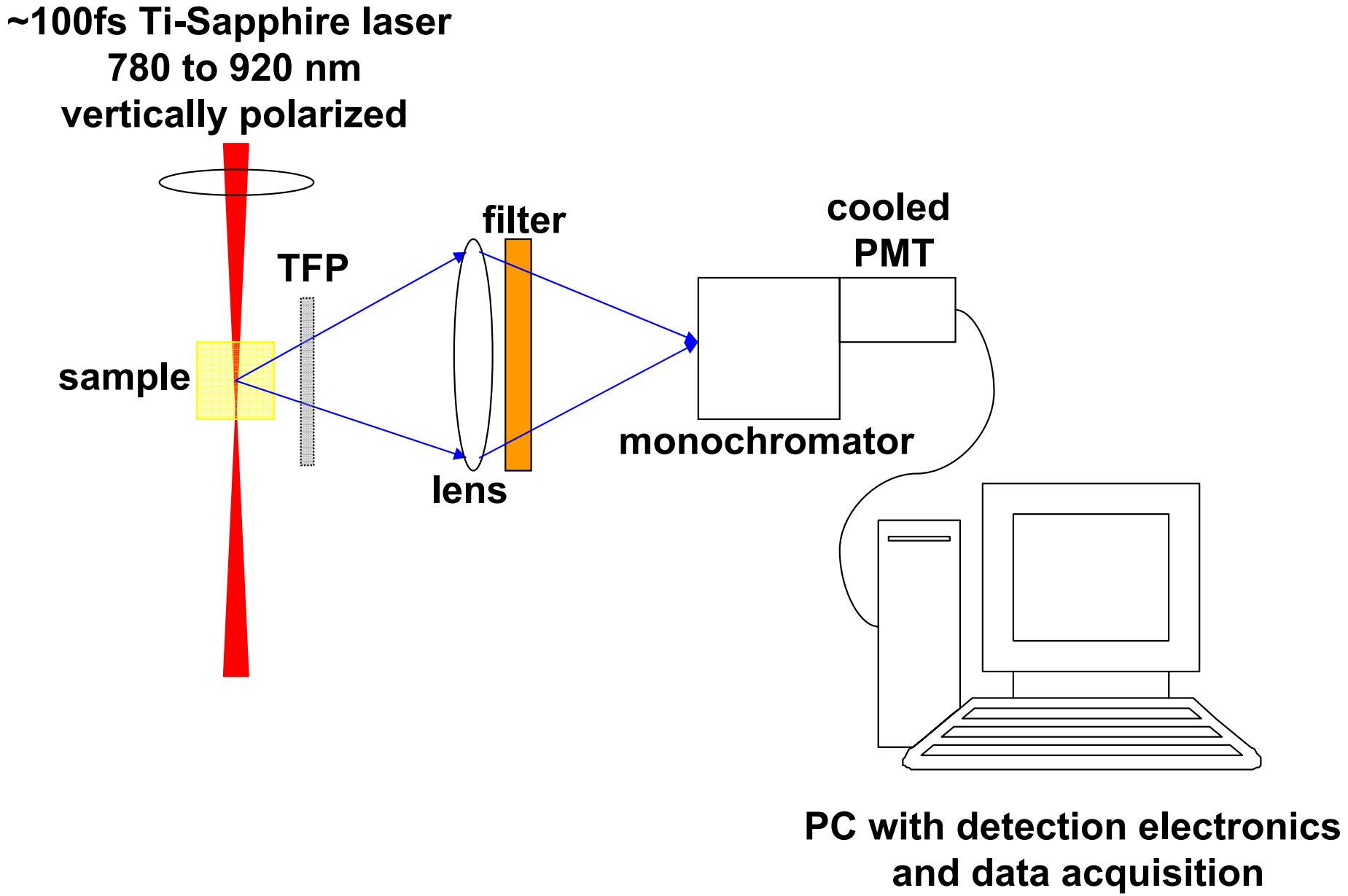

SH from Silver Nanoparticles

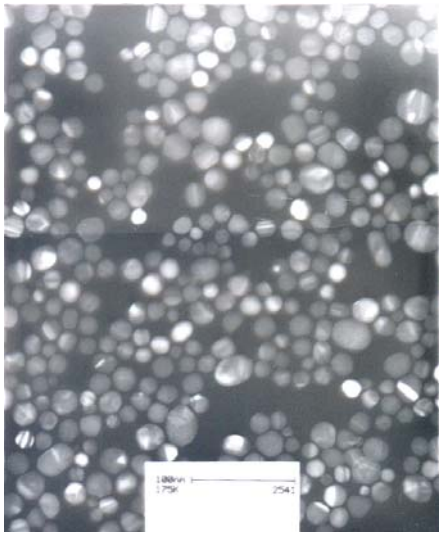

TEM picture

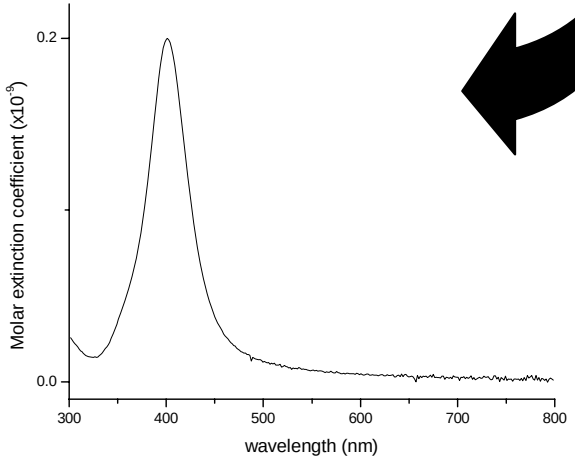

Typical extinction spectra

SH spectrum

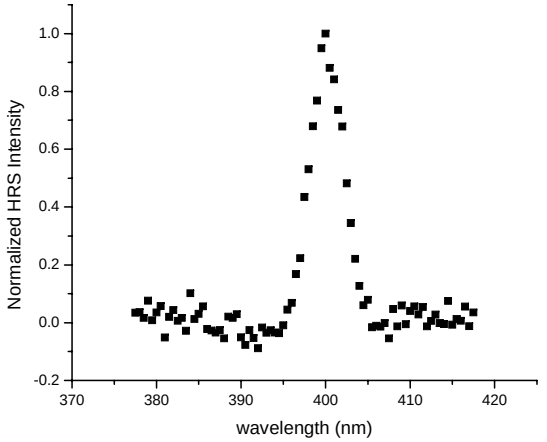

SH intensity vs. incident laser power

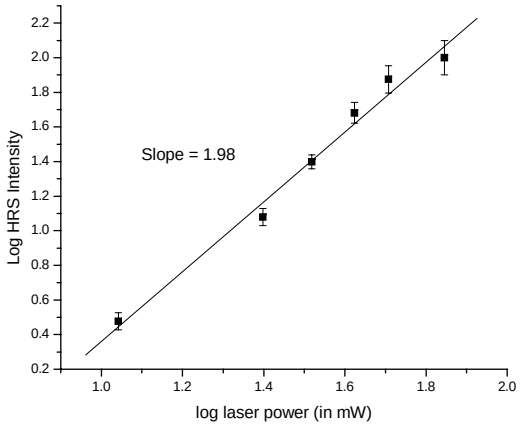

Excitation source:

Femtosecond laser @ 800 nm

Silver Nanoprisms

Preparation: Chemical method (Adv. Materials, 17, 2005, 412)

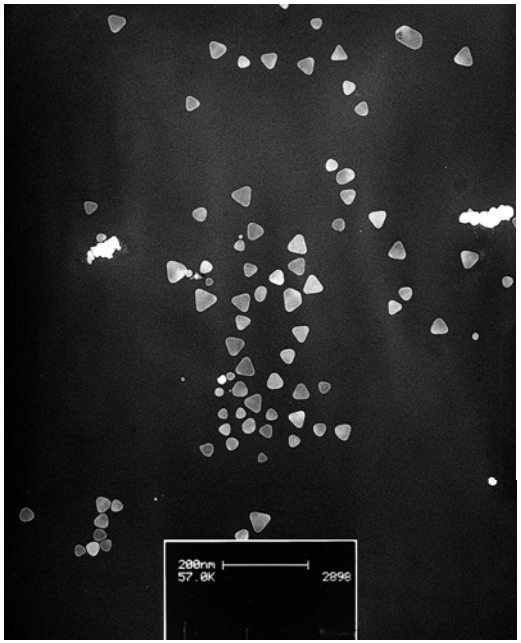

Typical TEM image of Silver nanoprisms

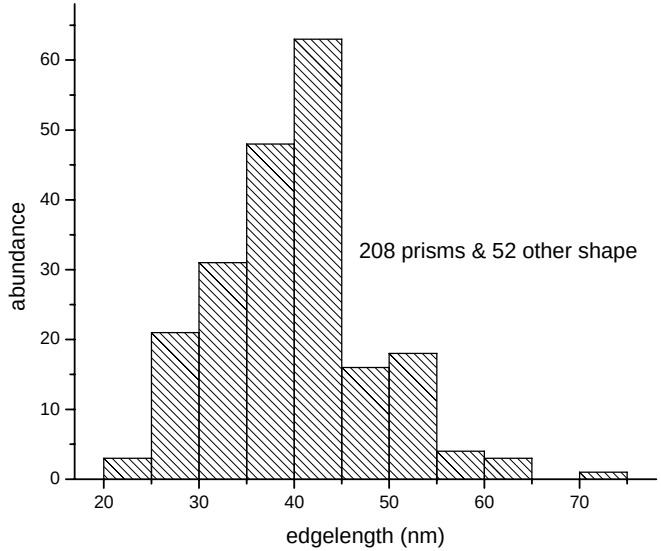

Histogram of the edge length distribution

Average edge length: 35-45 nm
Average thickness: 4-5 nm

Typical extinction spectrum

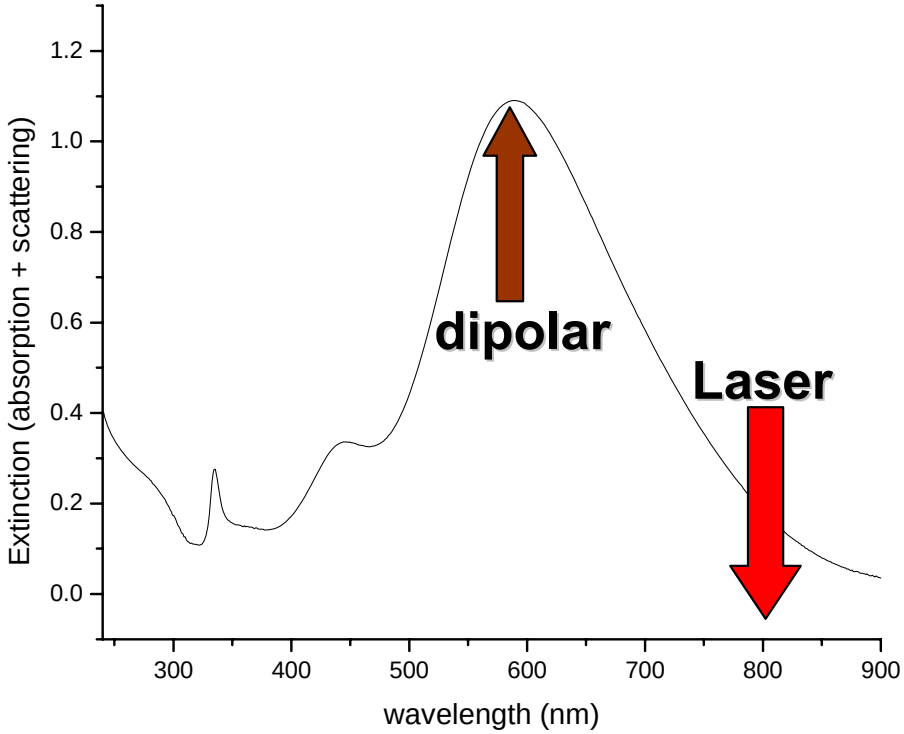

- **Dipolar SPR band is very sensitive to the environment**
- **Attractive candidate for various sensing applications**
- **Many of the sensing applications are based on ensemble average spectroscopic properties**
- **Important to study the ensemble spectroscopic properties of the nanoparticles alone**

Multiphoton absorption induced processes in Ag nanoprisms

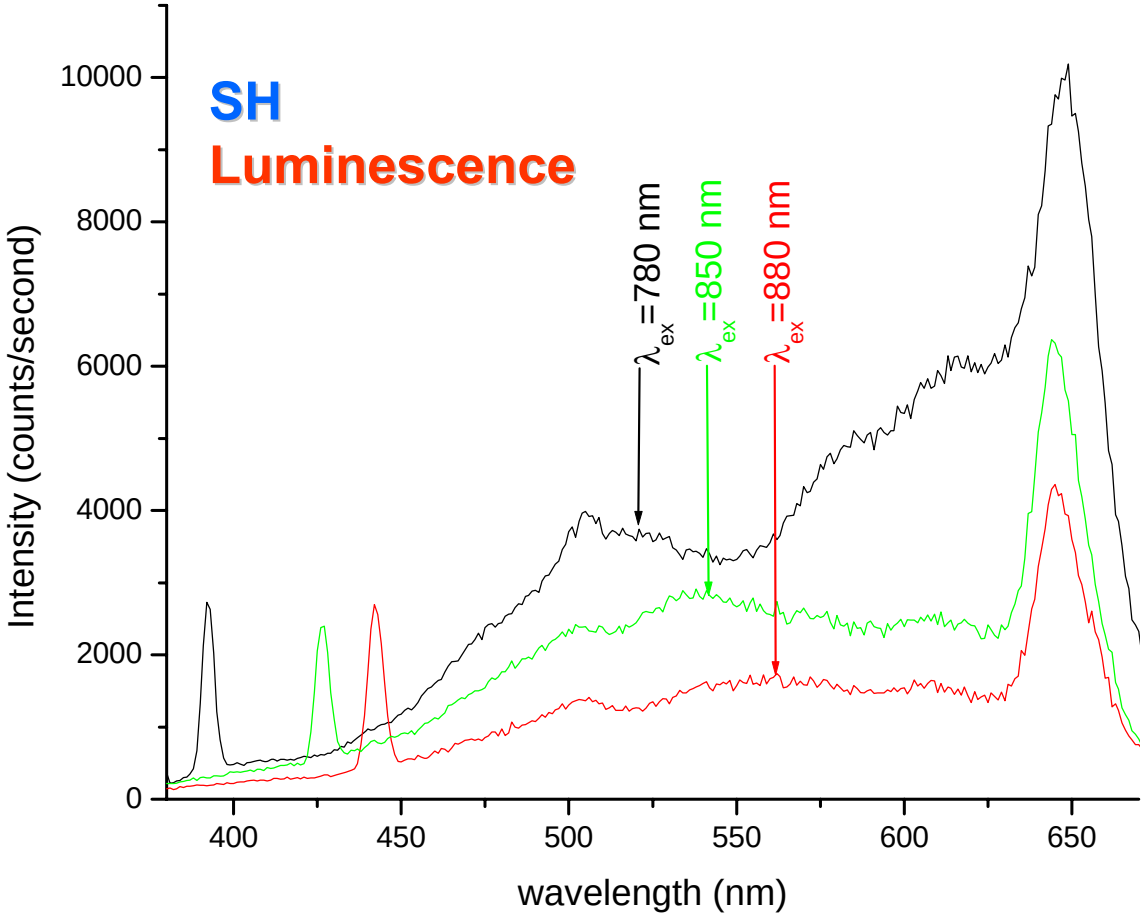

- Luminescence intensity excitation wavelength dependent
- The onset of luminescence precedes the SH peak

(> second order process??)

Power dependence of SH and luminescence

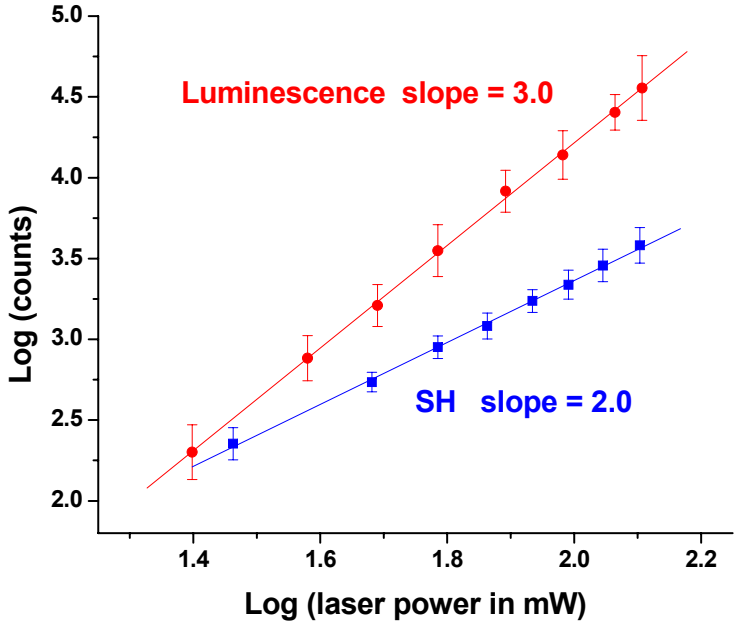

Luminescence from the silver nanoprisms is a three-photon induced process

- Coupling of incoming (excitation) and outgoing (luminescence) with localized surface plasmons
- Presence of sharp corners/tips where SP field is intense

Hyperpolarizability (β) measurement of spheres & prisms

$$I_{2\omega} = G < N_s \beta_s^{\ 2} + N_a \beta_a^{\ 2} > I_\omega^2 e^{(-N_a(2\alpha_\omega + \alpha_{2\omega})l)}$$

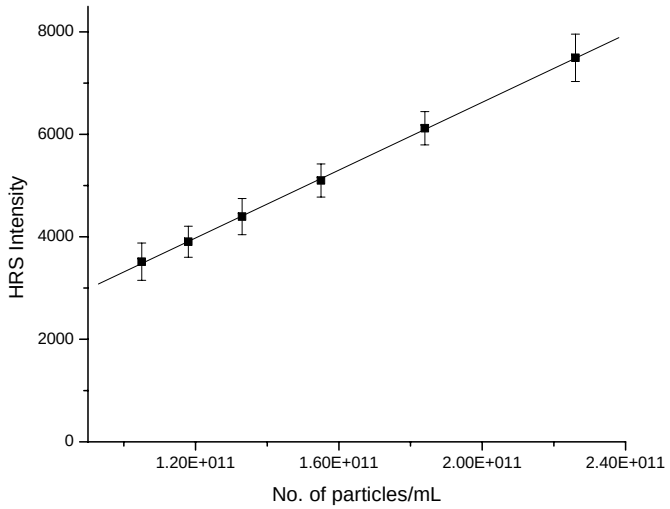

Prisms

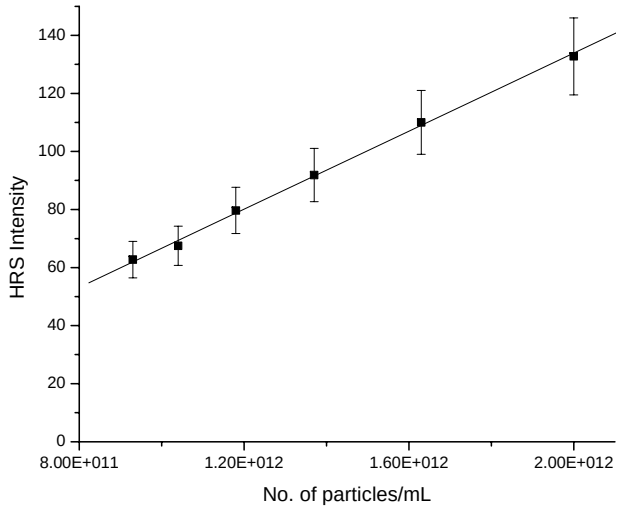

Spheres

For 850 nm excitation the β/ value for nanoprisms and spheres are 35000 ± 5000 x 10^{-30} esu and 2000 ± 800 x 10^{-30} esu respectively

Effect of addition of electrolytes on nanospheres

- Addition of salt reduces the thickness of Electrical Double Layer
- Reduces electrostatic repulsion
- Formation of aggregates
- Tremendous increase in β : enhanced SH (and SERS)

Salt effect on Ag Nanospheres

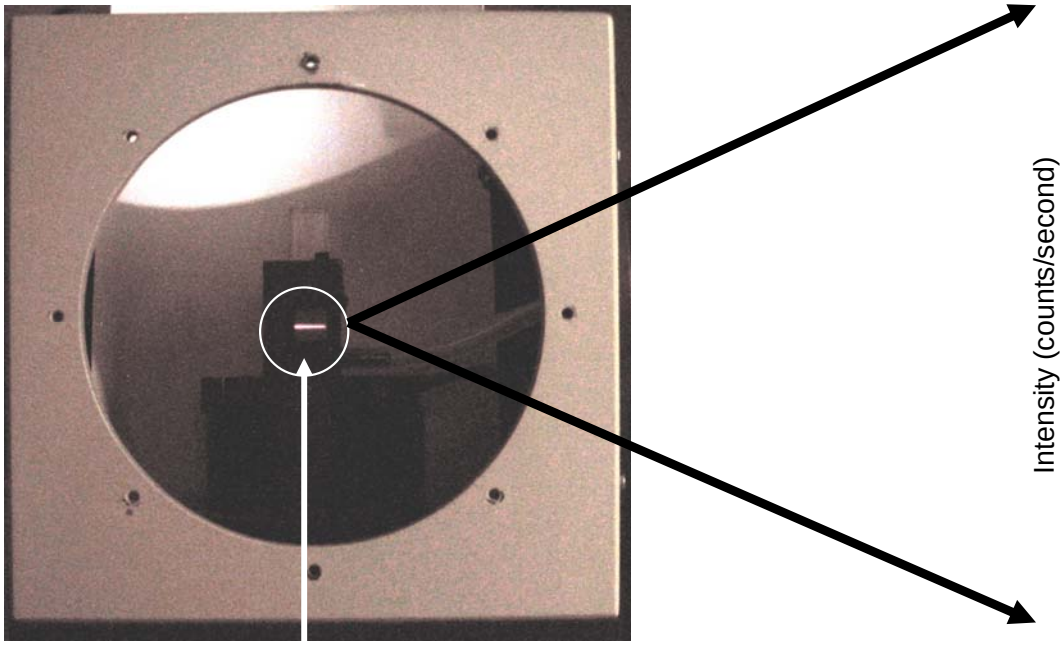

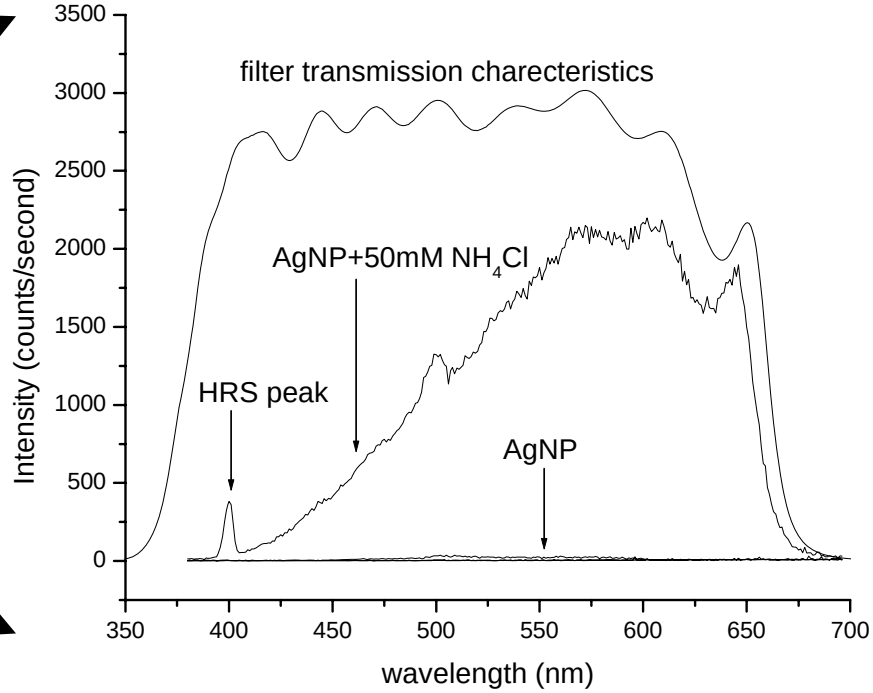

Ag Nanoparticles with 50 mM NH_4Cl

SH & luminescence from aggregated AgNPs

Relative SH enhancement: Salt effect

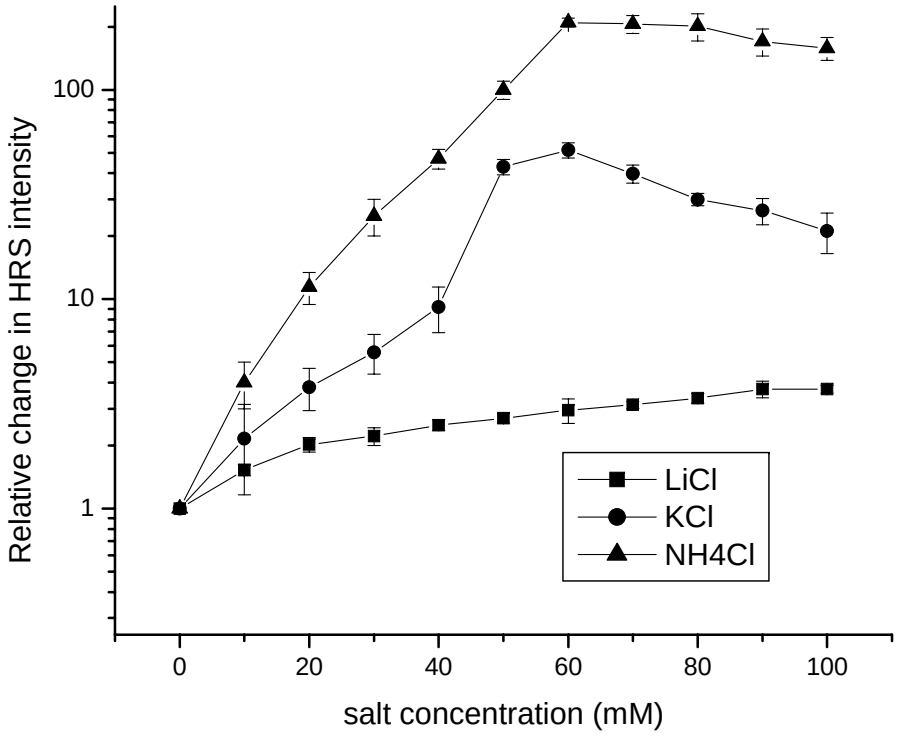

LiCl : ~4 times
KCl : ~50 times
NH_4Cl : ~200 times

$r_{Lithium} < r_{Pottasium} < r_{Ammonium}$

0.68 A⁰ 1.33 A⁰ 1.61 A⁰

Size and hence the charge density of the cation plays an important role in colloidal aggregation

Particle size distribution

w/o electrolyte

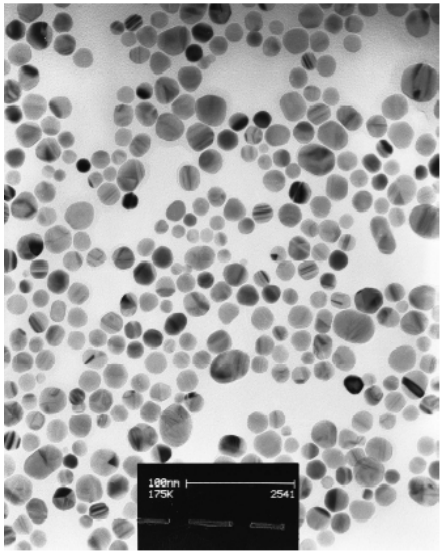

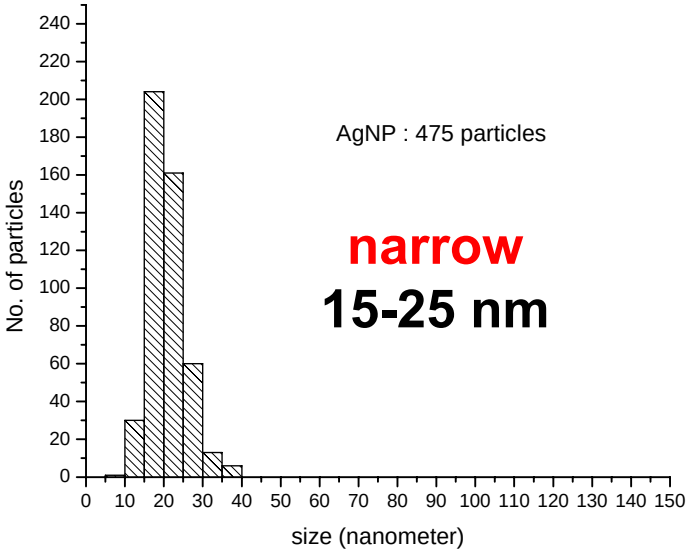

with electrolyte

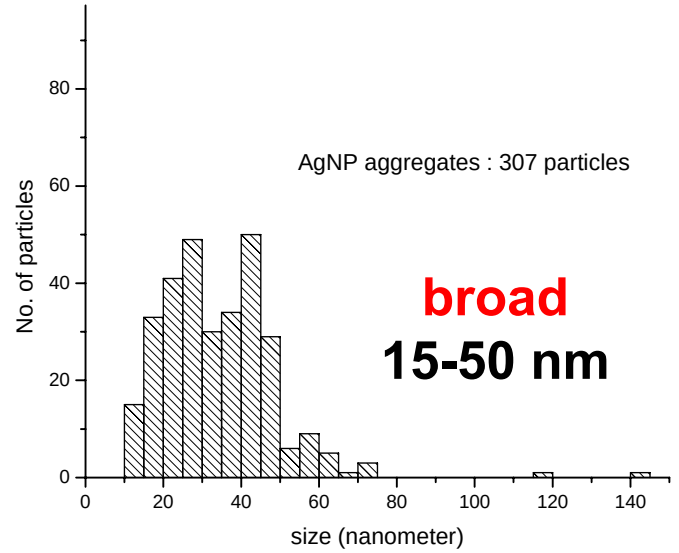

Time dependent change of SH intensity of NH_4Cl induced aggregates : Effect of addition of a polymer

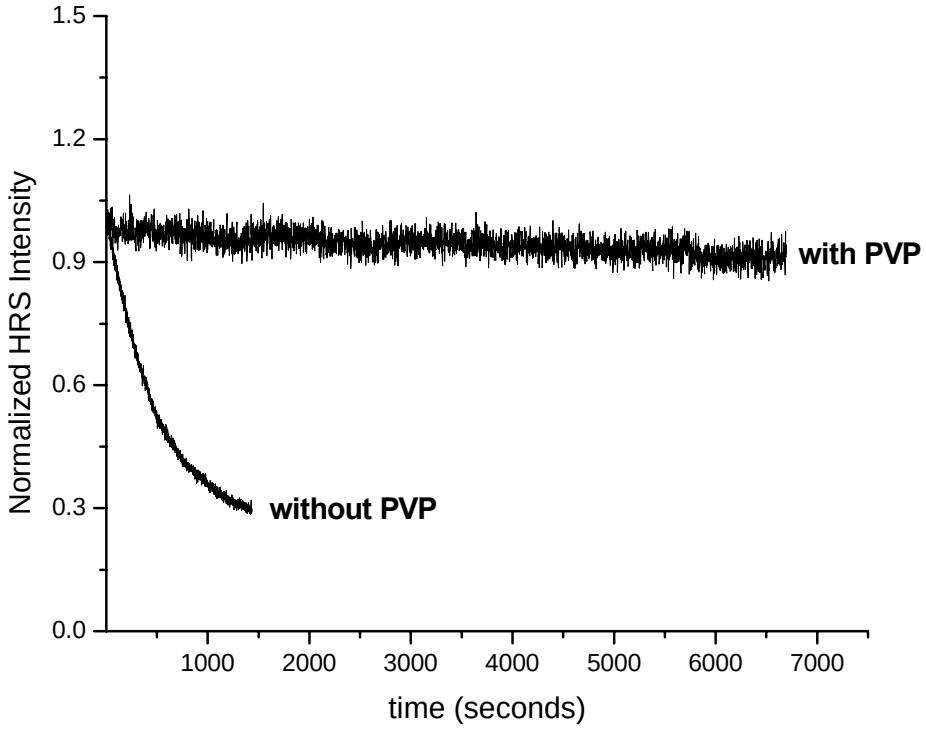

Addition of polymer, PVP stabilizes the SH signal

Excitation wavelength dependence of SH & luminescence of polymer stabilized NH_4Cl induced aggregates

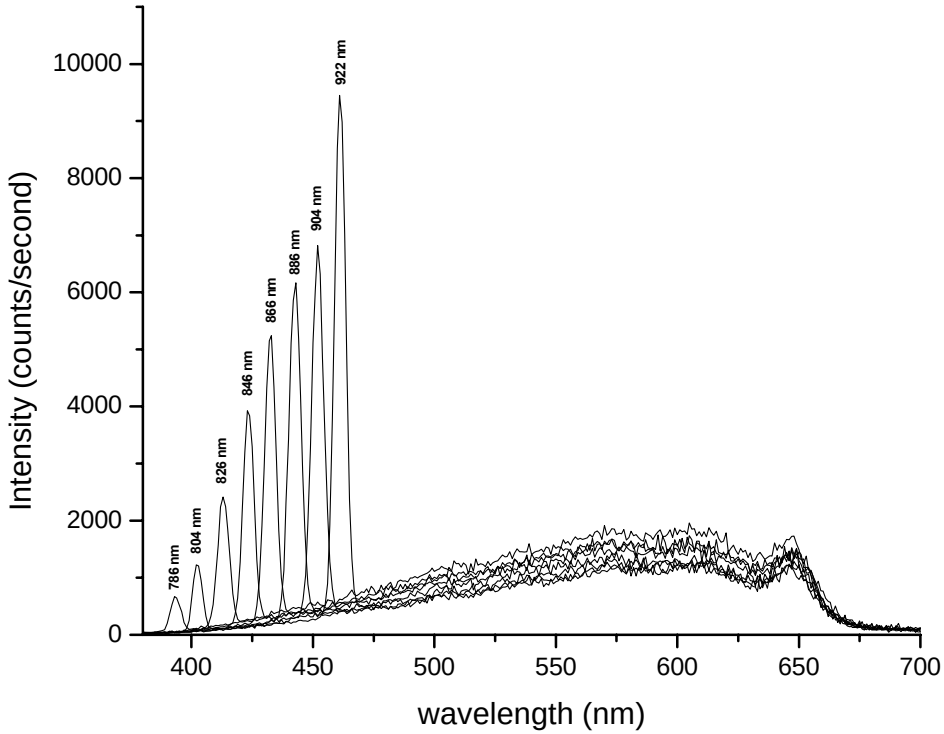

- SH intensities increase by ~ two orders of magnitude
- The luminescence however, remains more or less similar

Wavelength dependent SH intensity profile

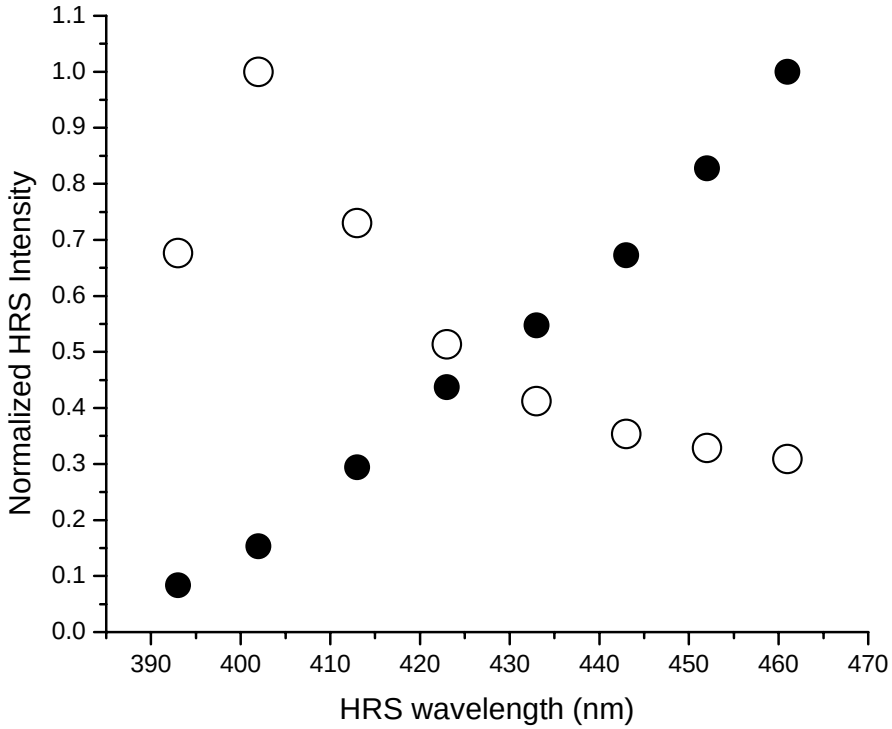

- Non-aggregated AgNPs resembles closely to their extinction spectra

- For aggregates, the SH intensity increases steadily with no apparent hint of a nearby maximum

Acknowledgement

Dr. B. Bose
B. Jain
Dr. A. Uppal

Thank you